NAS

A FEASIBILITY STUDY FOR

LASER WATER TURBIDI

by

G. D. Hickman
A. H. Ghovanlo
E. J. Friedman
C. S. Gault
J. E. Hogg

Prepared Under Contract No. NAS1-1225

SPARCOM, INC.
Alexandria, VA.

for

NATIONAL AERONAUTICS AND SPACE ADMINISTR

TABLE OF CONTENTS

ABSTRACT

A technique to remotely determine the attenuation coefficient (α) of the water was investigated. The backscatter energy ($\theta = 180°$) of a pulse laser ($\lambda = 440 - 660$ nm) was found directly related to the water turbidity for waters characterized by $\alpha \leq 6m^{-1}$. The greatest sensitivity was found to exist at 440 nm. For waters whose turbidity was adjusted using Chesapeake Bay sediment, the sensitivity in determining α at 440 nm was found to be approximately 5 - 10%. A correlation was also found to exist between the water depth (time) at which the peak backscatter occurs and α.

ACKNOWLEDGEMENT

The authors would like to acknowledge the able assistance of technician, Mr. Al Boshoff, who helped in performing the experiments in SPARCOM'S environmental tank.

Dr. Peter Mumola, NASA Langley, and Mr. Les Dunn, EPA, Las Vegas are gratefully acknowledged for serving as project monitors.

I. Introduction

Lasers[1,2,3] have been used to remotely measure properties of the water. Precise interpretation of the return laser signal(s) requires knowledge of the absorption and scattering coefficients of the water as a function of wavelength.

The quantity and type of sediment suspended in water determines the turbidity of the water and the transmission of electromagnetic energy in water. The results of a previous study showed that there was a direct correlation between the quantity, type of sediment and the optical attenuation coefficient (α) of water. The object of this study was to determine the feasibility of using the laser backscatter signal to remotely determine the attenuation coefficient of the water. If proven feasible, a device based on this measurement could be an integral portion of an airborne laser bathymetric surveillance system. In addition, it could be used to map the discharge of heavy sediment laden streams, etc, into larger bodies of water.

II. Optical Properties of Water

The attenuation coefficient (α) of the water is given by the equation

$$\alpha(\lambda) = a(\lambda) + s \qquad (1)$$

where $a(\lambda)$ is the absorption coefficient as a function of wavelength (λ). The parameter s is the scattering coefficient which for this study is considered to be independent of wavelength. For a collimated beam of light, the intensity (I) decreases, over a specified path length (x) when the photons are either scattered out of the beam or absorbed by the water. The intensity as a function of distance is given by the equation

$$I = I_o \, e^{-\alpha x} \tag{2}$$

where I_o is the initial intensity of the beam.

This attenuation coefficient can be obtained for different combinations of absorption and scattering coefficients. Thus, the parameter $a(\lambda)/s$ has been defined to characterize a particular type of sediment.

The scattering of light that occurs in each small volume of water is a basic parameter for the calculation of the backscattered signal. Equation (3) describes the radiant intensity at a given angle θ for unpolarized light in terms of the volume scattering function $\sigma(\theta)$

$$dI(\theta) = \sigma(\theta) \, I_o \, dv \tag{3}$$

where

I_o = irradiance produced by a collimated beam

dv = differential scattering volume

dI(θ) = radiant intensity at an angle θ

θ = angle with respect to forward direction of incident beam.

The scattering coefficient (s) is obtained by integrating the volume scattering function over the solid angled Ω (Equation 4).

$$s = \int \sigma(\theta)\, d\Omega = 2\pi \int_0^{\pi} \sigma(\theta)\, \sin\theta\, d\theta \qquad (4)$$

III. Experimental Measurements

The laser backscattered signal was measured in Sparcom's Environmental Water Tank using two sediments having different values of a/s*. The two sediments that were used to control the turbidity in the water tank were quartz (a/s = 0.06) and Chesapeake Bay sediment (a/s = 0.20). The wavelength of the laser light was varied from 440 to 660 nm in intervals of 20 nm. Figure 1 is a schematic diagram of the experimental set-up that was used to measure the backscattered signal.

An additional set of experiments were completed to correlate the attenuation coefficient with Secchi disk measurements. The latter are commonly used for measurement of turbidity. Appendix A contains some details on the use and limitations of Secchi disk measurements.

The beam from the pulsed dye laser entered the Environ-

*a/s ratios were measured at 540 nm.

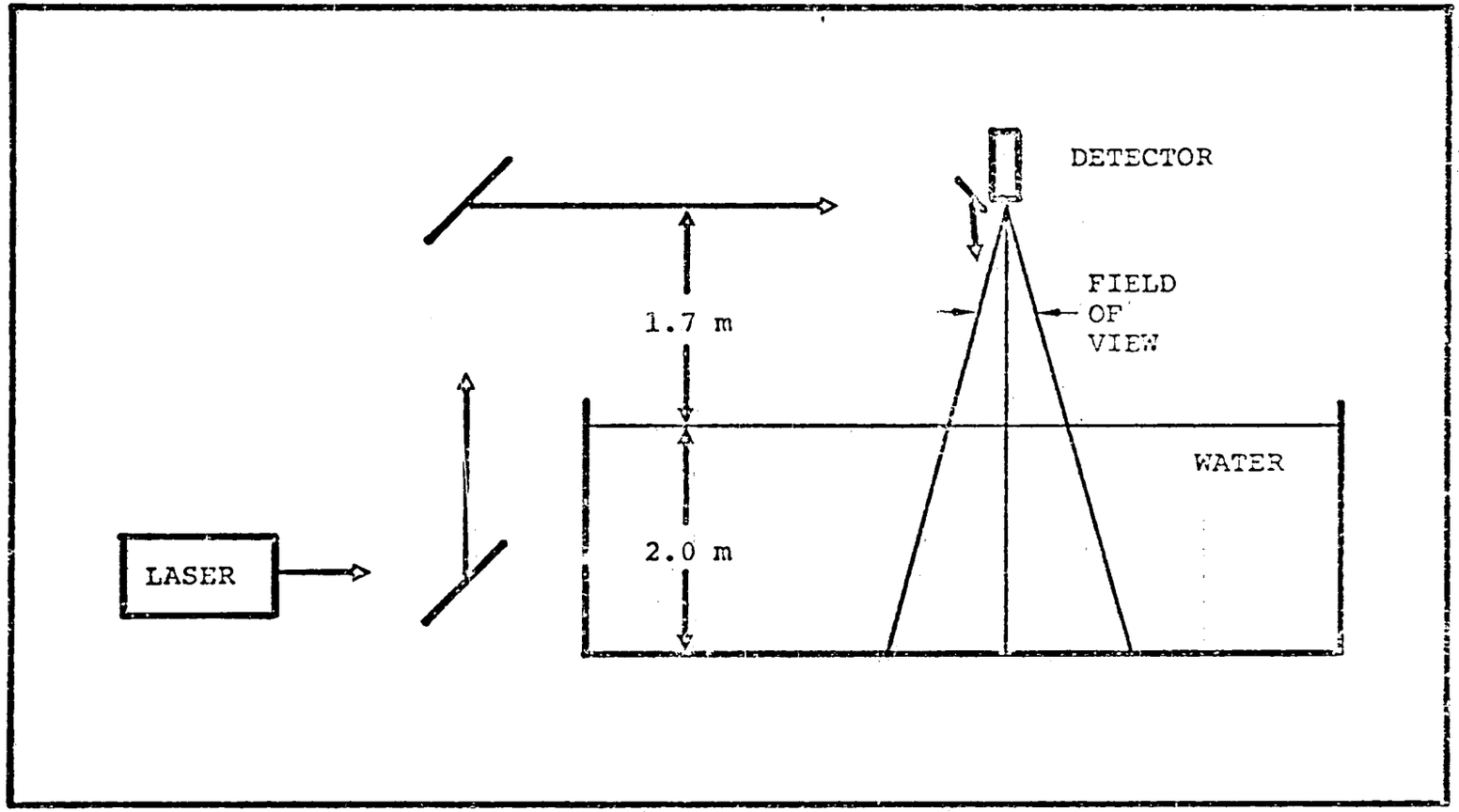

Figure 1: A schematic diagram of the experimental set-up that was used to measure the backscattered signal.

mental Tank from above the water as shown in Figure 1. The photomultiplier tube (PMT) viewed the laser backscattered signal from 1.7 meters above the water. Detection of the direct surface reflection was avoided by tilting the detector approximately 2° with respect to normal incidence of the laser beam.

The effect of possible interfering surface and bottom reflections on the backscatter signal was investigated. This was accomplished by placing highly reflective surfaces both on the water surface and the bottom. It was discovered that the slight tilt on the detectors, as previously mentioned was sufficient to avoid reflections from the highly specular water surface. For clear shallow water ($\alpha \leq 0.5\ m^{-1}$) the backscatter is small in relation to the bottom signal. However, for values of $\alpha \geq 1.0\ m^{-1}$ the backscatter becomes the predominate term and is easily distinguished from the bottom signal.

The present set of experiments was performed for quiescent waters. Future experiments should be designed to investigate the effect of capillary waves on the backscatter signal.

A series of experiments were performed to measure the shape, the maximum amplitude and the depth of water from which the backscattered laser pulse is generated. These measurements were also performed as a function of the de-

tector's field of view. As previously mentioned, the wavelength of the laser was varied from 440 - 660 nm. The results of the quartz measurements are summarized in Tables I and II for an input laser power of 1 watt. The results of similar type experiments using Chesapeake Bay sediment are summarized in Tables III and IV. Figure 2 shows sampling backscattered signals for a wavelength of 540 nm from turbidities characterized by α values ranging from 1.0 - 6.0 m^{-1}. These results were obtained for quartz induced turbidities with a 200 mrad. field of view detector. However, the shape of the curves are very similar to those obtained for the Chesapeake Bay sediments. They were found to be independent of the detector field of view. The amplitude of the pulse shown in Figure 2 cannot be compared as they were observed using various detector sensitivities.

The relation between the amplitude of the peak backscattered signal and the attenuation coefficient α is demonstrated in Figure 3 for the case where Chesapeake Bay sediment is used to control the water turbidity. Data are shown for four different wavelengths (λ = 440, 480, 500 and 560 nm) for a detector having a 200 mrad. field of view. Figure 4 shows similar type data for the case where the turbidity of the water was controlled by quartz particles. The curves shown in Figures 3 and 4 represent a best fit to the experimental numbers. It should be noted that in all cases the α

Laser Wavelength nm	Detector Field of View [mrad]	Peak Detected Laser Backscattered Signal [watts]* Turbidity (α) m^{-1} α = 0.5	α = 1.0	α = 2.0	α = 4.0	α = 6.0
440	50	9.2×10^{-4}	8.3×10^{-4}	1.2×10^{-3}	1.1×10^{-3}	1.7×10^{-3}
	100	9.6×10^{-4}	1.4×10^{-3}	2.3×10^{-3}	1.9×10^{-3}	3.4×10^{-3}
	200	1.8×10^{-3}	2.3×10^{-3}	4.0×10^{-3}	6.0×10^{-3}	7.0×10^{-3}
	400	2.0×10^{-3}	2.8×10^{-3}	4.7×10^{-3}	3.8×10^{-3}	7.8×10^{-3}
460	50	5.2×10^{-4}	9.5×10^{-4}	1.3×10^{-3}	2.0×10^{-3}	2.1×10^{-3}
	100	8.4×10^{-4}	1.3×10^{-3}	1.9×10^{-3}	3.2×10^{-3}	3.1×10^{-3}
	200	1.6×10^{-4}	2.6×10^{-3}	3.4×10^{-3}	5.2×10^{-3}	4.9×10^{-3}
	400	1.9×10^{-4}	3.2×10^{-3}	4.2×10^{-3}	7.0×10^{-3}	6.5×10^{-3}
480	50	5.6×10^{-4}	8.4×10^{-4}	1.1×10^{-3}	1.4×10^{-3}	2.3×10^{-3}
	100	9.0×10^{-4}	1.1×10^{-3}	1.9×10^{-3}	2.1×10^{-3}	3.0×10^{-3}
	200	1.5×10^{-3}	2.0×10^{-3}	3.8×10^{-3}	3.8×10^{-3}	4.6×10^{-3}
	400	1.8×10^{-3}	2.8×10^{-3}	4.7×10^{-3}	4.7×10^{-3}	5.8×10^{-3}
500	50	5.6×10^{-4}	8.4×10^{-4}	1.0×10^{-3}	1.9×10^{-3}	1.7×10^{-3}
	100	7.5×10^{-4}	1.1×10^{-3}	1.5×10^{-3}	2.4×10^{-3}	2.6×10^{-3}
	200	1.7×10^{-3}	2.1×10^{-3}	2.2×10^{-3}	3.8×10^{-3}	4.5×10^{-3}
	400	2.0×10^{-3}	2.4×10^{-3}	2.7×10^{-3}	4.5×10^{-3}	5.4×10^{-3}
520	50	5.6×10^{-4}	7.2×10^{-4}	1.2×10^{-3}	1.4×10^{-3}	1.5×10^{-3}
	100	7.1×10^{-4}	9.6×10^{-4}	1.6×10^{-3}	2.0×10^{-3}	2.3×10^{-3}
	200	1.4×10^{-3}	1.9×10^{-3}	2.4×10^{-3}	3.4×10^{-3}	3.1×10^{-3}
	400	1.9×10^{-3}	2.0×10^{-3}	2.9×10^{-3}	4.0×10^{-3}	4.1×10^{-3}
540	50	5.7×10^{-4}	7.2×10^{-4}	1.1×10^{-3}	1.5×10^{-3}	2.2×10^{-3}
	100	6.2×10^{-4}	9.0×10^{-4}	1.5×10^{-3}	2.0×10^{-3}	3.0×10^{-3}
	200	1.4×10^{-3}	1.6×10^{-3}	2.2×10^{-3}	2.9×10^{-3}	4.5×10^{-3}
	400	1.6×10^{-3}	1.9×10^{-3}	2.7×10^{-3}	3.5×10^{-3}	5.8×10^{-3}

*Normalized to a one watt input laser signal.

Table I - Peak Laser Backscattered Signal as a Function of Wavelength and Water Turbidity. Quartz was used to control the turbidity.

Laser Wavelength nm	Detector Field of View [mrad]	Peak Detected Laser Backscattered Signal [watts]* Turbidity (α) m^{-1}				
		$\alpha = 0.5$	$\alpha = 1.0$	$\alpha = 2.0$	$\alpha = 4.0$	$\alpha = 6.0$
560	50	6.7×10^{-4}	6.7×10^{-4}	9.0×10^{-4}	1.1×10^{-3}	1.4×10^{-3}
	100	7.5×10^{-4}	1.0×10^{-3}	1.3×10^{-3}	1.6×10^{-3}	2.5×10^{-3}
	200	1.3×10^{-3}	1.6×10^{-3}	2.0×10^{-3}	2.7×10^{-3}	3.7×10^{-3}
	400	1.5×10^{-3}	1.9×10^{-3}	2.2×10^{-3}	3.2×10^{-3}	4.7×10^{-3}
580	50	5.1×10^{-4}	4.6×10^{-4}	9.0×10^{-4}	1.1×10^{-3}	1.8×10^{-3}
	100	6.7×10^{-4}	7.5×10^{-4}	1.3×10^{-3}	1.6×10^{-3}	2.5×10^{-3}
	200	1.0×10^{-3}	1.2×10^{-3}	1.7×10^{-3}	2.4×10^{-3}	3.8×10^{-3}
	400	1.2×10^{-3}	1.3×10^{-3}	2.0×10^{-3}	3.2×10^{-3}	4.7×10^{-3}
600	50	4.7×10^{-4}	5.2×10^{-4}	7.2×10^{-4}	1.3×10^{-3}	1.6×10^{-3}
	100	5.4×10^{-4}	6.6×10^{-4}	9.8×10^{-4}	1.5×10^{-3}	2.2×10^{-3}
	200	9.7×10^{-4}	1.3×10^{-3}	1.7×10^{-3}	2.2×10^{-3}	3.5×10^{-3}
	400	1.1×10^{-3}	1.4×10^{-3}	2.0×10^{-3}	2.7×10^{-3}	4.4×10^{-3}
620	50	4.6×10^{-4}	5.1×10^{-4}	9.0×10^{-4}	9.7×10^{-4}	1.3×10^{-3}
	100	7.4×10^{-4}	6.7×10^{-4}	1.1×10^{-3}	1.5×10^{-3}	2.2×10^{-3}
	200	1.1×10^{-3}	1.2×10^{-3}	1.7×10^{-3}	2.2×10^{-3}	3.5×10^{-3}
	400	1.3×10^{-3}	1.4×10^{-3}	2.0×10^{-3}	2.7×10^{-3}	4.0×10^{-3}
640	50	5.1×10^{-4}	5.1×10^{-4}	9.0×10^{-4}	1.2×10^{-3}	1.4×10^{-3}
	100	6.8×10^{-4}	6.8×10^{-4}	1.2×10^{-3}	1.7×10^{-3}	2.3×10^{-3}
	200	1.0×10^{-3}	1.1×10^{-3}	1.9×10^{-3}	2.6×10^{-3}	3.6×10^{-3}
	400	1.2×10^{-3}	1.2×10^{-3}	2.4×10^{-3}	3.0×10^{-3}	3.8×10^{-3}
660	50	3.7×10^{-4}	4.5×10^{-4}	8.2×10^{-4}	9.8×10^{-4}	1.1×10^{-3}
	100	4.5×10^{-4}	5.5×10^{-4}	1.1×10^{-3}	1.3×10^{-3}	1.7×10^{-3}
	200	9.2×10^{-4}	9.2×10^{-4}	2.5×10^{-3}	1.7×10^{-3}	2.4×10^{-3}
	400	1.0×10^{-4}	1.0×10^{-4}	3.0×10^{-3}	2.0×10^{-3}	3.2×10^{-3}

*Normalized to a one watt input laser signal.

Table II - Peak Laser Backscattered Signal as a Function of Wavelength and Water Turbidity. Quartz was used to control the turbidity.

Laser Wavelength nm	Detector Field of View [mrad]	Peak Detected Laser Backscattered Signal [watts]* — Turbidity (α) m^{-1}						
		α = 0.08	α = 0.30	α = 0.48	α = 0.98	α = 1.9	α = 4.0	α = 6.0
440	50	1.0×10^{-3}	9.0×10^{-4}	8.8×10^{-4}	1.7×10^{-3}	3.4×10^{-3}	4.9×10^{-3}	9.0×10^{-3}
	100	1.3×10^{-3}	1.2×10^{-3}	1.3×10^{-3}	2.5×10^{-3}	5.3×10^{-3}	6.4×10^{-3}	1.2×10^{-2}
	200	2.6×10^{-3}	2.0×10^{-3}	1.8×10^{-3}	3.8×10^{-3}	8.0×10^{-3}	14.0×10^{-3}	1.8×10^{-2}
	400	2.9×10^{-3}	2.2×10^{-3}	2.4×10^{-3}	4.5×10^{-3}	1.5×10^{-2}	1.8×10^{-2}	2.5×10^{-2}
460	50	4.3×10^{-4}	9.0×10^{-4}	1.1×10^{-3}	1.8×10^{-3}	2.3×10^{-3}	2.7×10^{-3}	
	100	5.5×10^{-4}	1.2×10^{-3}	1.4×10^{-3}	2.1×10^{-3}	3.0×10^{-3}	3.8×10^{-3}	
	200	1.0×10^{-3}	2.0×10^{-3}	2.0×10^{-3}	3.1×10^{-3}	4.0×10^{-3}	6.0×10^{-3}	
	400	1.1×10^{-3}	2.4×10^{-3}	2.4×10^{-3}	3.6×10^{-3}	4.6×10^{-3}	7.2×10^{-3}	
480	50	4.2×10^{-4}	6.8×10^{-4}	1.1×10^{-3}	1.8×10^{-3}	2.9×10^{-3}	4.7×10^{-3}	5.9×10^{-3}
	100	8.4×10^{-4}	1.0×10^{-3}	1.6×10^{-3}	2.3×10^{-3}	3.4×10^{-3}	6.5×10^{-3}	9.2×10^{-3}
	200	1.2×10^{-3}	2.4×10^{-3}	2.4×10^{-3}	3.0×10^{-3}	4.5×10^{-3}	1.0×10^{-2}	1.2×10^{-2}
	400	1.4×10^{-3}	2.9×10^{-3}	2.6×10^{-3}	3.3×10^{-3}	5.5×10^{-3}	1.2×10^{-2}	1.4×10^{-2}
(6) 500	50	3.5×10^{-4}	6.5×10^{-4}	8.5×10^{-4}	1.7×10^{-3}	2.5×10^{-3}	4.1×10^{-3}	
	100	5.0×10^{-4}	9.5×10^{-4}	1.0×10^{-3}	2.1×10^{-3}	3.5×10^{-3}	5.0×10^{-3}	
	200	1.4×10^{-3}	1.8×10^{-3}	1.6×10^{-3}	2.8×10^{-3}	4.5×10^{-3}	7.3×10^{-3}	
	400	1.9×10^{-3}	2.2×10^{-3}	2.1×10^{-3}	3.5×10^{-3}	5.6×10^{-3}	9.7×10^{-3}	
520	50	3.0×10^{-4}	6.8×10^{-4}	9.6×10^{-4}	1.6×10^{-3}	3.0×10^{-3}	3.4×10^{-3}	
	100	3.5×10^{-4}	9.6×10^{-4}	1.3×10^{-3}	2.2×10^{-3}	3.5×10^{-3}	4.5×10^{-3}	
	200	6.5×10^{-4}	1.4×10^{-3}	1.6×10^{-3}	2.9×10^{-3}	4.7×10^{-3}	6.0×10^{-3}	
	400	9.8×10^{-4}	1.7×10^{-3}	2.0×10^{-3}	3.1×10^{-3}	5.2×10^{-3}	8.6×10^{-3}	
540	50	2.5×10^{-4}	4.5×10^{-4}	6.9×10^{-4}	1.2×10^{-3}	1.4×10^{-3}	3.1×10^{-3}	3.4×10^{-3}
	100	3.0×10^{-4}	6.9×10^{-4}	9.3×10^{-4}	1.4×10^{-3}	1.9×10^{-3}	4.1×10^{-3}	4.8×10^{-3}
	200	6.5×10^{-4}	8.7×10^{-4}	1.3×10^{-3}	2.1×10^{-3}	2.5×10^{-3}	4.8×10^{-3}	6.4×10^{-3}
	400	8.1×10^{-4}	1.0×10^{-3}	1.5×10^{-3}	2.2×10^{-3}	3.2×10^{-3}	5.8×10^{-3}	7.4×10^{-3}

*Normalized to a one watt input laser signal.

Table III - Peak Laser Backscattered Signal as a Function of Wavelength and Water Turbidity. Chesapeake Bay Sediment was used to control the turbidity.

Laser Wavelength nm	Detector Field of View [mrad]	Peak Detected Laser Backscattered Signal [watts]* Turbidity (α) m^{-1} α = 0.08	α = 0.30	α = 0.48	α = 0.98	α = 1.9	α = 4.0	α = 6.0
560	50	3.5×10^{-4}	4.8×10^{-4}	6.8×10^{-4}	1.3×10^{-3}	2.0×10^{-3}	2.9×10^{-3}	
	100	5.0×10^{-4}	7.5×10^{-4}	9.5×10^{-4}	1.6×10^{-3}	2.5×10^{-3}	4.0×10^{-3}	
	200	1.0×10^{-3}	9.8×10^{-4}	1.5×10^{-3}	2.1×10^{-3}	3.2×10^{-3}	5.5×10^{-3}	
	400	1.4×10^{-3}	1.1×10^{-3}	1.5×10^{-3}	2.4×10^{-3}	4.2×10^{-3}	6.2×10^{-3}	
580	50	2.5×10^{-4}	4.9×10^{-4}	8.0×10^{-4}	9.0×10^{-4}	1.8×10^{-3}	2.7×10^{-3}	
	100	3.5×10^{-4}	7.5×10^{-4}	1.2×10^{-3}	1.4×10^{-3}	2.5×10^{-3}	3.2×10^{-3}	
	200	6.5×10^{-4}	1.2×10^{-3}	1.7×10^{-3}	1.9×10^{-3}	3.3×10^{-3}	4.2×10^{-3}	
	400	9.0×10^{-4}	1.4×10^{-3}	2.0×10^{-3}	2.2×10^{-3}	4.0×10^{-3}	5.4×10^{-3}	
600	50	2.4×10^{-4}	4.0×10^{-4}	5.7×10^{-4}	9.6×10^{-4}	1.5×10^{-3}	2.0×10^{-3}	3.7×10^{-3}
	100	4.9×10^{-4}	5.3×10^{-4}	7.4×10^{-4}	1.2×10^{-3}	2.1×10^{-3}	2.7×10^{-3}	5.4×10^{-3}
	200	8.0×10^{-4}	9.2×10^{-4}	1.5×10^{-3}	1.7×10^{-3}	2.4×10^{-3}	3.6×10^{-3}	7.6×10^{-3}
	400	1.2×10^{-3}	1.1×10^{-3}	1.3×10^{-3}	2.0×10^{-3}	2.8×10^{-3}	4.2×10^{-3}	8.5×10^{-3}
620	50	2.2×10^{-4}	4.0×10^{-4}	6.0×10^{-4}	9.0×10^{-4}	1.5×10^{-3}	2.7×10^{-3}	
	100	3.5×10^{-4}	5.4×10^{-4}	8.0×10^{-4}	1.2×10^{-3}	2.1×10^{-3}	3.3×10^{-3}	
	200	1.1×10^{-3}	1.0×10^{-3}	1.3×10^{-3}	1.6×10^{-3}	3.4×10^{-3}	4.2×10^{-3}	
	400	1.3×10^{-3}	1.2×10^{-3}	1.4×10^{-3}	1.9×10^{-3}	3.8×10^{-3}	5.0×10^{-3}	
640	50	2.0×10^{-4}	4.6×10^{-4}	4.4×10^{-4}	7.9×10^{-4}	1.4×10^{-3}	2.5×10^{-3}	4.2×10^{-3}
	100	3.2×10^{-4}	5.2×10^{-4}	5.1×10^{-4}	1.1×10^{-3}	1.9×10^{-3}	3.4×10^{-3}	5.8×10^{-3}
	200	7.9×10^{-4}	9.2×10^{-4}	1.2×10^{-3}	1.6×10^{-3}	2.4×10^{-3}	4.3×10^{-3}	7.7×10^{-3}
	400	9.2×10^{-4}	1.1×10^{-3}	1.0×10^{-3}	1.6×10^{-3}	2.8×10^{-3}	5.0×10^{-3}	9.3×10^{-3}

*Normalized to a one watt input laser signal.

Table IV - Peak Laser Backscattered Signal as a Function of Wavelength and Water Turbidity. Chesapeake Bay Sediment was used to control the turbidity.

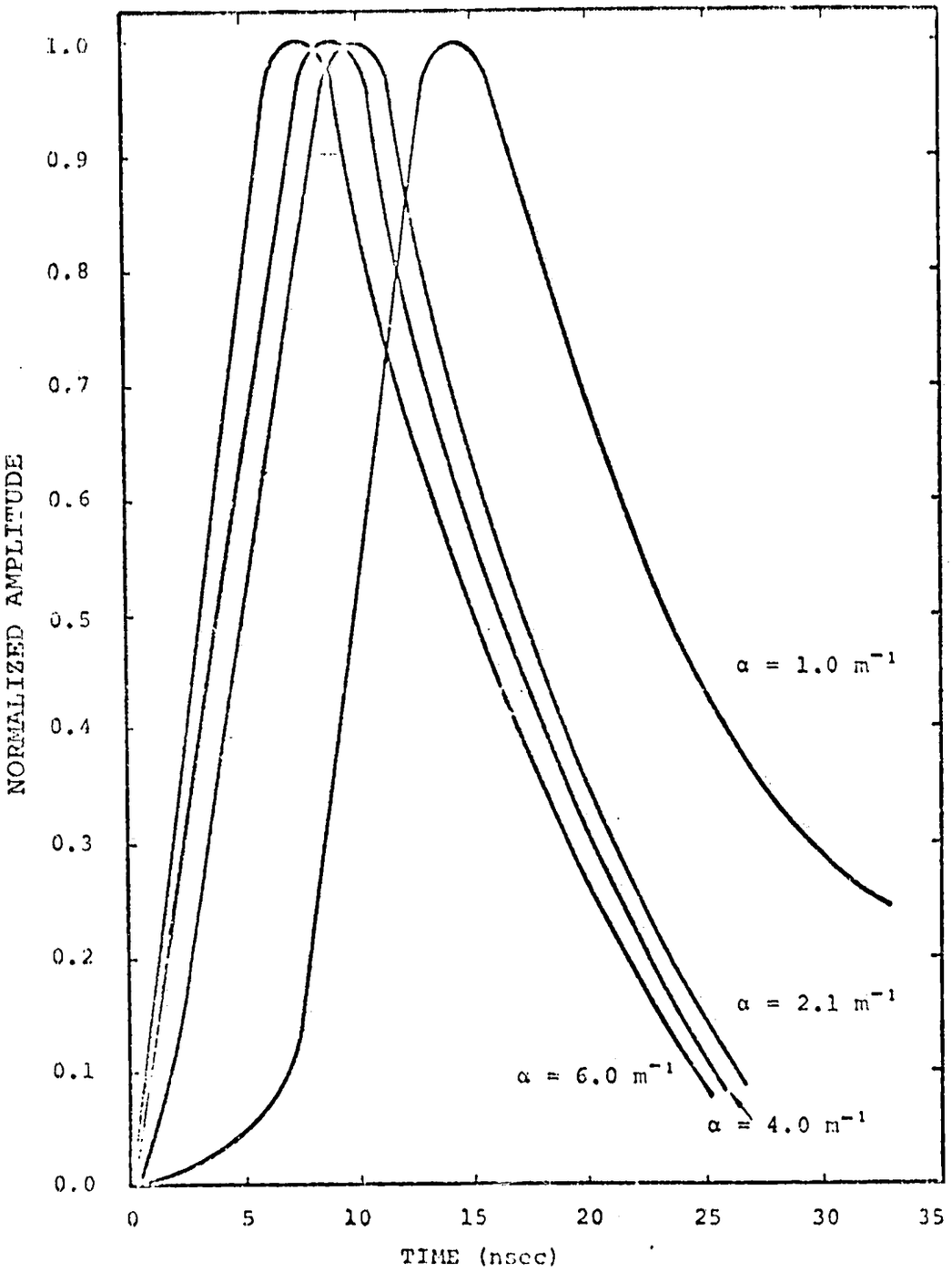

Figure 2: The shape of the backscattered signal as a function of α using quartz to change the turbidity.

and a values have been measured at 540 nm. Measurements are currently in progress to determine the wavelength dependence of both α and a in the wavelength region of 440 to 660 nm. These results will be used to correct the α values given in this report. The shape of the curves in Figures 3 and 4 are basically the same except that the slopes are appreciably steeper for the natural sediment, thereby resulting in better sensitivity.

In order to compare the behavior of the various curves shown in Figures 3 and 4 a quantity R_x has been defined as

$$R_x = \frac{\text{peak backscattered signal @ } \alpha = 6.0 \text{ m}^{-1}}{\text{peak backscattered signal @ } \alpha = 0.5 \text{ m}^{-1}} \qquad (5)$$

where x represents the particular particles used to simulate the water turbidity, i.e.,

$$x = s \text{ (Chesapeake Bay sediment)}$$

$$= q \text{ (quartz particles)}$$

Table V gives the values of $R_s(\lambda)$ and $R_q(\lambda)$ for wavelengths of 440 to 660 nm.

λ (nm)	440	480	500	560	580	600	620	660
$R_s(\lambda)$	10.0	5.00	5.44	4.86	-	6.00	-	-
$R_q(\lambda)$	3.89	3.13	2.64	2.74	3.80	3.50	3.50	2.40

Table V: Ratio of peak backscattered signals for different wavelengths.

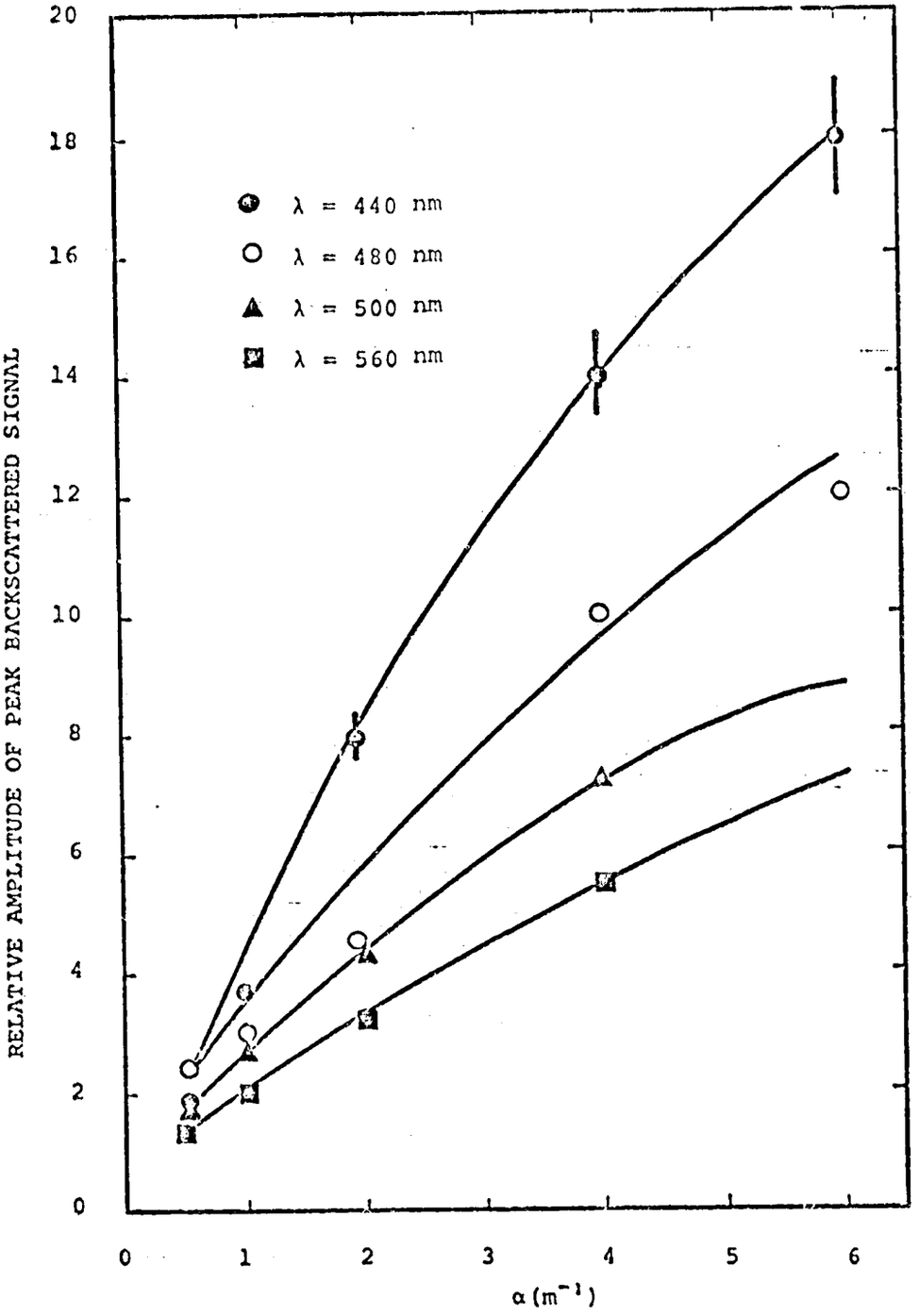

Figure 3: The amplitude of the peak backscattered signal is shown as a function of α for various wavelengths. The turbidity was adjusted using Chesapeake Bay sediment.

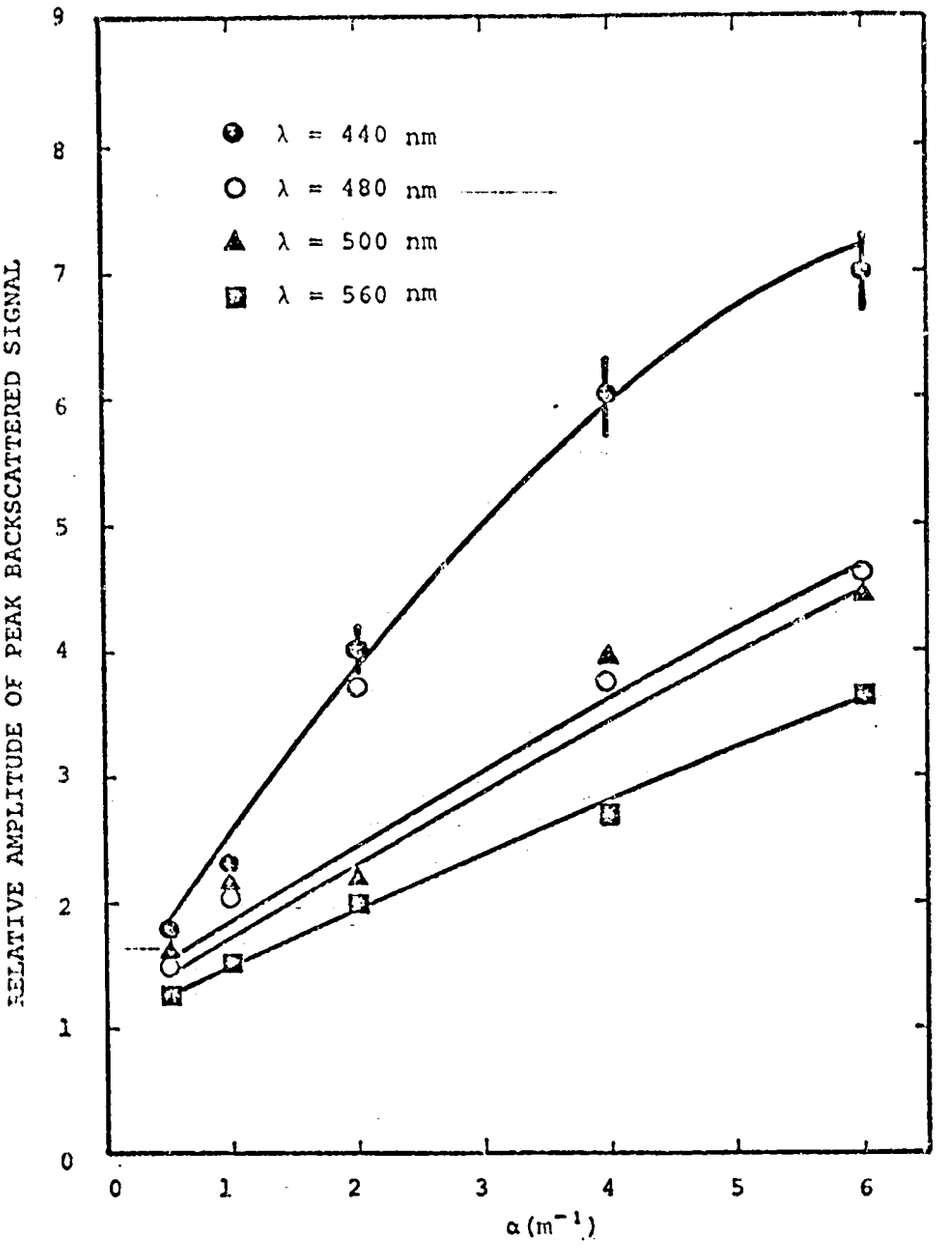

Figure 4: The amplitude of the peak background signal is shown as a function of α for various wavelengths. The turbidity was adjusted using quartz.

The results given in Table V show that the backscatter/α curve exhibits a positive slope for all wavelengths. This means that the backscatter signal from any wavelength in the 440 - 660 nm region could be used as a measurement of α. For both quartz and natural sediment the slopes of the curves are approximately the same for all wavelengths, except at 440 nm. The slope of the backscatter curve at the latter wavelength is substantially greater. A laser operating at this wavelength would be the most sensitive to changes in α, thereby making it the best α detector. The sensitivity of this technique, using the wavelength of 440 nm, is estimated from Figure 3 to be approximately 5 - 10%. A laser operating at still a lower wavelength may result in increased sensitivity.

It has been established that in some underwater applications the use of polarization techniques reduces the backscattered signal and improves the contrast.[5] An experiment was performed to measure the effect of polarization on the backscattered signal as a function of turbidity. The laser beam was linearly polarized using one polarizer in front of the laser output while a second polarizer was placed in front of the detector. By changing the relative angle of the two polarizers, the amplitude of the backscattered signal could be maximized or minimized. It was determined experimently that there was no correlation between the ratio L

$$L = \frac{\text{amplitude of the maximum signal}}{\text{amplitude of the minimum signal}}$$

and the turbidity of the water.

IV. Analytical Model

The shape of the laser backscattered signal and the time at which its peak response occurs in the water is predicted using a one dimensional model for the experimental geometry shown in Figure 5. This model is designed to examine the primary features of the backscattering problem for the case of a pulsed laser. Additional calculations are needed to develop a three dimensional analytical model for the prediction of the detailed shape and the magnitude of the backscattered signal.

At a time $t = 0$, a short pulse is propagated towards the water and impinges on the air/water interface at a time $t = D/c$ where D is the distance between the laser/detector system and the air/water interface. Consider the case for which the front edge of the pulse is at position x and the entire pulse is in the water. The parameter τ fixes a point within the pulse. The amplitude of the signal detected at a time $2t$, $f(2t)$, neglecting the difference between the velocity of light in air and water, is given by

$$f(2t) = \int_{\tau=0}^{L/2c} g(2\tau)\ P(\lambda; t-\tau)\ d\tau \qquad (6)$$

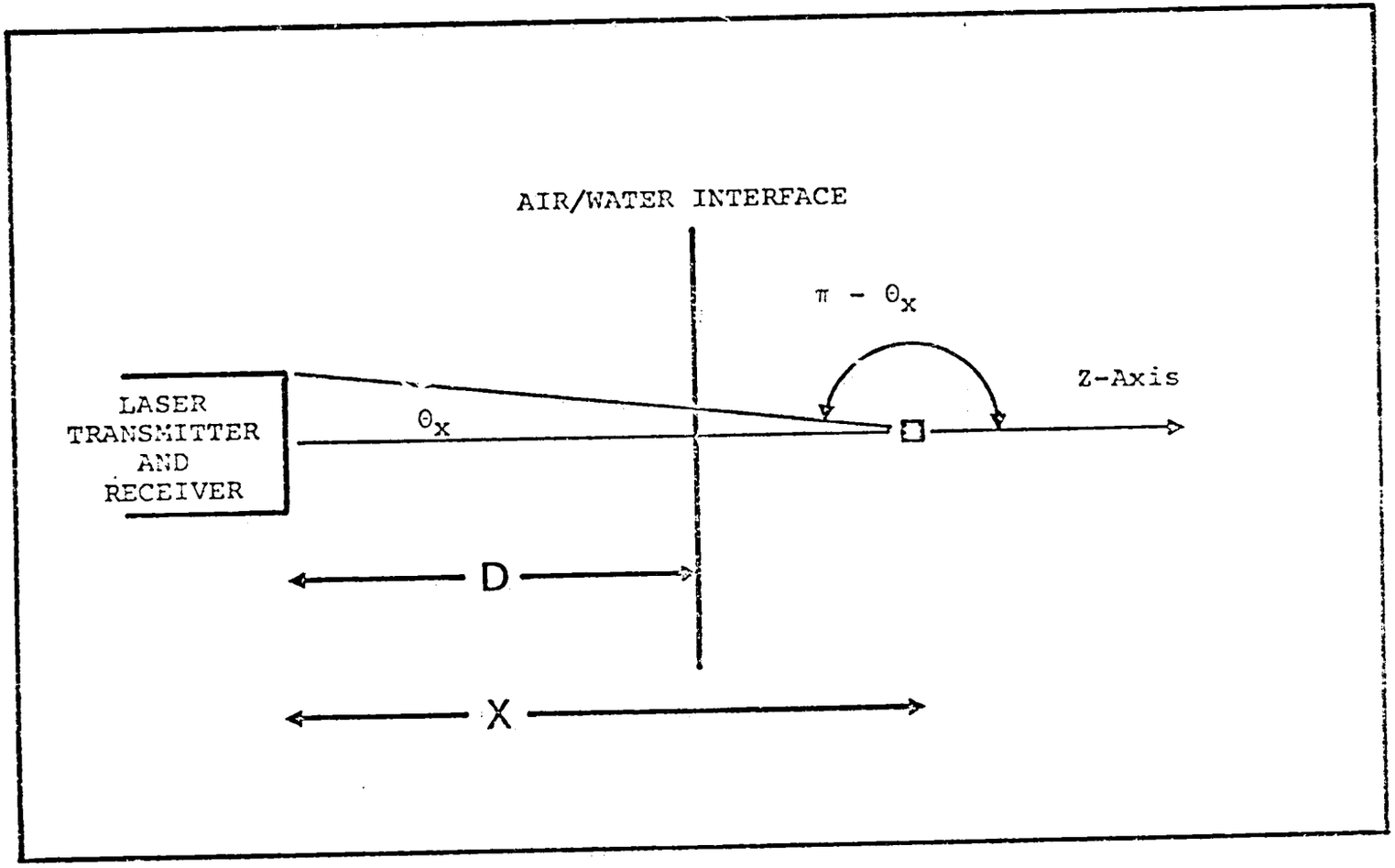

Figure 5. A schematic diagram of the experimental set-up used to measure the backscattered signal.

for

$$t \geq (D+L)/c \qquad \text{and}$$

$$f(2t) = \int_{\tau=0}^{L'/2c} g(2\tau)\ P\ (\lambda; t-\tau)\ d\tau \tag{7}$$

for $\qquad (D+L)/c \geq t \geq D/c \qquad$ and $0 < L' < L$

where L is the length of the pulse.

$$f\ (2t) \equiv 0 \qquad \text{for } t < D/c \tag{8}$$

$g(\tau)$ is the power distribution function for the pulse. The peak amplitude of the pulse occurs at τ_m such that $g\ (\tau_m) \equiv 1$ and the peak power is $P_o g(\tau_m)/L$. $P(\lambda; t-\tau)$ is the response function of the sediment which is reponsible for the generation of the backscattered signal.

The response function $P(\lambda; x)$ is derived for a line element located at a point x as shown in Figure 5.

$$dP(\lambda; x) = (P_o/L)\ e^{-2\alpha_\lambda (x-D)}\ \sigma(\lambda; \pi)\ d\Omega \tag{9}$$

which upon integration yields

$$P(\lambda; x) = (P_o/L)\ e^{-2\alpha_\lambda (x-D)}\ \sigma(\lambda; \pi)\ 2\pi\left(1 - \frac{x}{(a^2+x^2)^{1/2}}\right) \tag{10}$$

where a is the radius of the detector. The exponential term accounts for the attenuation of the signal in the water while $\sigma(\lambda;\pi)$ is the volume scattering function at 180 degrees.

Inserting equation (10) into equation (6) results in the following expression for the detected signal as a function of α_λ and wavelength, i.e.,

$$f(2t) = (P_o/L)\ 2\pi c\ \sigma(\lambda;\pi)\ e^{-2\alpha_\lambda c(t-D/c)}\ I(t) \tag{11}$$

where

$$I(t) = \int_0^{\lambda/2;(t-D/c)/2} d\tau\ g(2\tau)\ e^{2\alpha_\lambda c\tau} \left\{1 - \frac{c(t-\tau)}{(a^2+c^2(t-\tau)^2)^{1/2}}\right\} \tag{12}$$

with $\gamma = L/C$. The upper limits of I (t) refer to the case $(\gamma/2)$ when the whole pulse is in the water or when part of the pulse ($[t-D/c]/2$) is in the water. The modified Gaussian pulse shape given by equation (13) is assumed for the power distribution function $g(\tau)$ which is inserted into equation (12).

$$g(\tau) = \left\{\frac{e}{e-1}\ (e^{-(2\tau/\gamma-1)^2} - e^{-1})\right\}^2 \tag{13}$$

The return laser signal has been calculated by numerically integrating equation (12). Appendix B describes the program

for the numerical integration. The results of the calculations for D = 1.7 meters, a detector radius (a) of 0.5 cm and α values ranging from 1 - 4 m^{-1} are shown in Figure 6. The value of $\sigma(\lambda;\pi)$ was assumed to be equal to 1 since the value of this function for the simulated waters was unknown. As the value of α is increased the peak of the backscattered signal shifts toward the surface of the water. It should be noted that these curves only show the shift of the peak with time. The relative amplitudes have not been normalized and therefore the various curves cannot be compared in amplitude. Table VI lists the time displacement of the pulse with respect to the water surface

α (m^{-1})	1	2	3	4
Time displacement of pulse (nsec)	5.8	4.7	3.9	3.4

Table VI: Time displacement (nsec) of the backscattered pulse for various values of α and γ = 6.0 nsec.

The experimental pulse shapes shown in Figure 2 show the same time shift as those displayed in Figure 6. Figure 7 shows the comparison between the experimental and calculated time shift as a function of α. Two calculated curves are presented; γ = 6 nsec, γ = 5.5 nsec. One observes that a definite correlation exists between the water depth at which the peak backscattering occurs (time

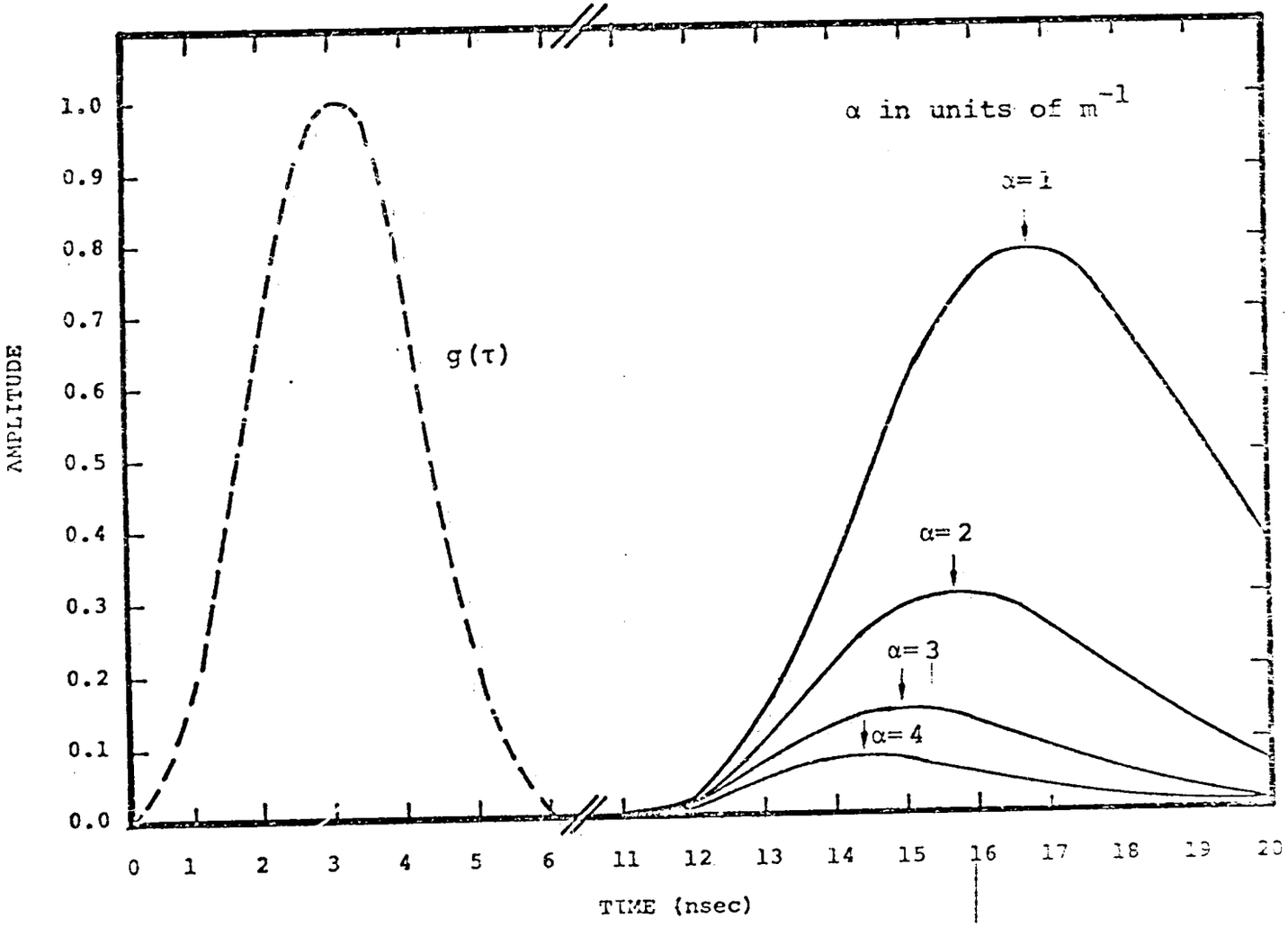

Figure 6: Calculation of the peak of the backscattered signal as a function of α and time. (The amplitudes of these curves have not been normalized)

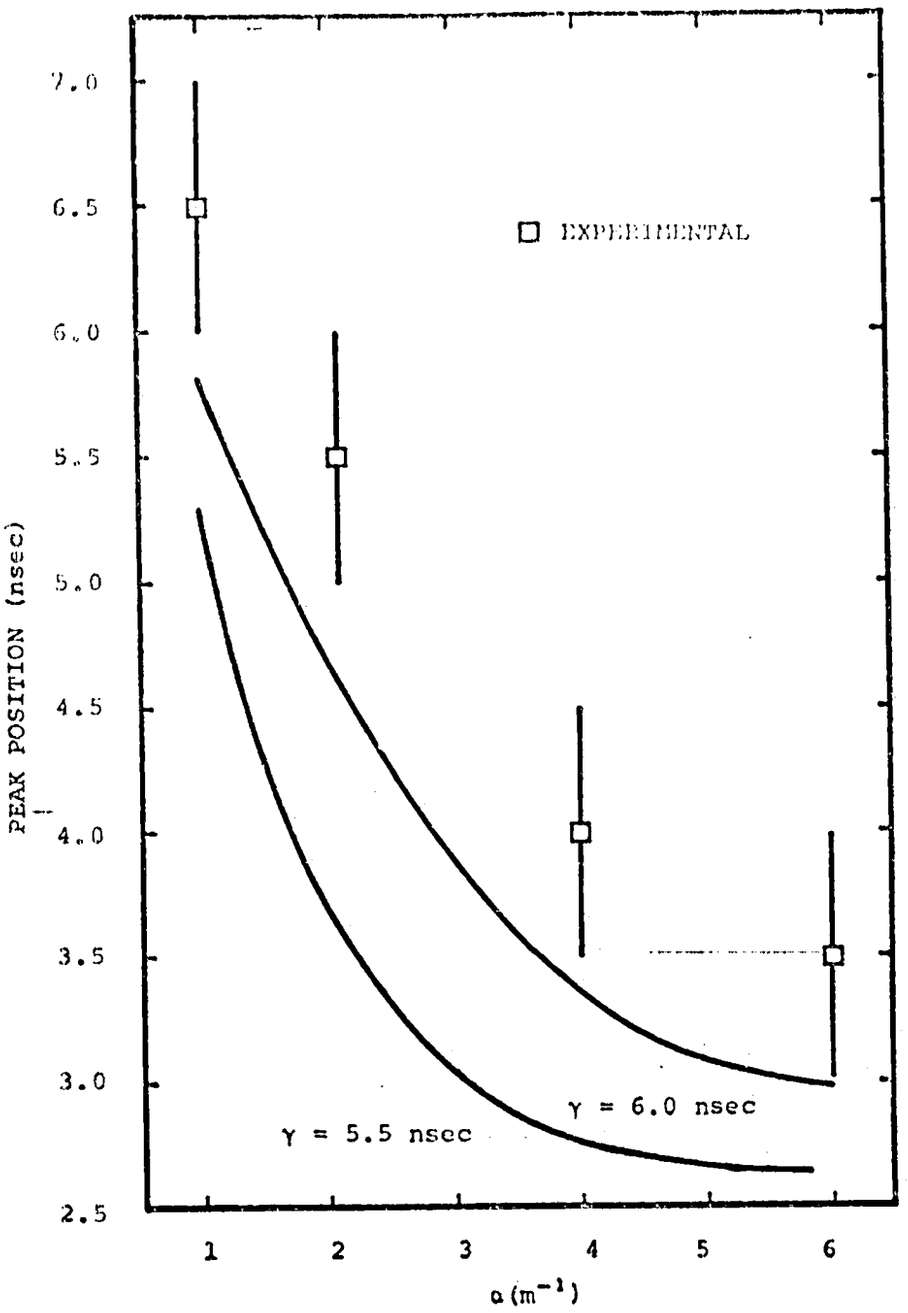

Figure 7: Comparison between the experimental and calculated time displacement of the peak backscattered signal.

displacement) and the water turbidity (α). In addition, good agreement is seen to exist between the calculated and experimental points.

V. Summary

A series of experiments were performed in which the laser backscatter energy was measured as a function wavelength and water turbidity. A tunable dye laser was used to vary the laser emission from 440 to 660 nm. The turbidity of the water was changed in discrete steps for values of the optical attenuation coefficient $\alpha \leq 6\ m^{-1}$. This was obtained by adding quartz and Chesapeake Bay sediment to the water in SPARCOM'S environmental-water tank facility.

The results showed a definite dependence of the backscatter energy with the attenuation coefficient (α) at all wavelengths. However, the strongest dependence of the backscattered signal on α was observed at 440 nm. The dependence on α was the same for both sediments, however, it was more pronounced for the Chesapeake Bay sediment. At an operating laser wavelength of 440 nm it is estimated that the attenuation coefficient (α) can be determined to within 5 - 10% in Chesapeake Bay type waters.

It was also shown that the peak of the backscattered energy occurred at a distance in the water corresponding to a two-way time path of 2.5 - 5.5 nsecs. The peak shifted towards shorter times, i.e., shallower depths as the water

turbidity increased. A one dimensional analytical model was formulated which was able to predict both the absolute time peaking and shift of the backscattered signal.

The initial calculations and measurements have shown that it may be feasible to use the laser signal backscattered from the near surface of the water as a remote sensing tool of water turbidity.

Although the backscatter is very sensitive to α, it may not be possible to design a system to measure the absolute value of α by detecting the laser backscatter at a single wavelength. However, it appears that a technique could be developed that is based on detecting the ratio of the laser backscatter at two or more wavelengths. Where applicable, a ratio technique can be extremely useful in that the majority of the system parameters cancel out. Additional measurements at various wavelengths, along with more detailed calculations are required in order to arrive at a ratio technique that can be used to determine α on an absolute basis.

Appendix A - Measurement of Water Turbidity

The optical properties of turbid water can be uniquely determined by use of two active light measuring instruments; an alpha (α) meter and an absorption (a) meter. The α-meter measures the total transmission loss of a light beam in water due to absorption and scattering, while the a-meter measures the loss due only to absorption.

Instead of using the above devices, which are relatively expensive and tedious to use, oceanographers for years have relied mainly upon Secchi disk readings for determination of visibility. While the Secchi disk is inexpensive, it is also less accurate than the active devices and is much more susceptible to errors produced by weather conditions and operator interpretations.

The Secchi disk[6] is a diffuse white target of radius r and reflectance ρ_D that disappears from view at a depth D in the water. The visibility of the disk is determined by the contrast between the disk and the background given by

$$\text{Contrast} = \frac{\text{Disk Brightness - Background}}{\text{Background}} \qquad \text{A.1}$$

The background light reaching the eye is the result of surface reflection and upwelling light. The background irradiance from the surface (B_s) is given by the equation

$$B_s = \rho_s E_o + \frac{uE_o(1-\rho_s)^2}{\pi} \qquad A.2$$

where

ρ_s = surface reflectance

E_o = incident intensity of light

u = fraction of incident radiation scattered upward

The background irradiance produced at a depth D is given by the equation

$$B_D = u\, E_o\, e^{-kD}\, (1-\rho_s)/\pi \qquad A.3$$

where

k = diffuse extinction coefficient.

The flux from the disk at depth D is

$$\phi_D = E_o\, (1-\rho_s)\, \rho_D\, d^{-kD}/\pi \qquad A.4$$

where

ρ_D = reflection from the target at depth D

and is attenuated by a factor of

$$e^{-\alpha D}\, (1-\rho_s)/(D^2+r^2).$$

Thus, the total flux from the disk that reaches the eye of the observer is given by

$$\Theta_D = \frac{E_o\, (1-\rho_s)^2\, \rho_D\, e^{-(k+\alpha)D}}{\pi\, (D^2+r^2)} \qquad A.5$$

From the equation A.1, the contrast at a depth D (C_D) is given by

$$C_D = \frac{\Phi_D - B_D}{B_D} \qquad \text{A.6}$$

or

$$C_D = \frac{\rho_D - u}{u} \qquad \text{A.7}$$

However, the contrast seen by the eye is given by

$$C_{eye} = C_D \left\{ \frac{B_D}{B_s} (1-\rho_s) \, e^{-\alpha D} \right\} \qquad \text{A.8}$$

in which the bracket represents the attenuation of the contrast of a submerged object.

If the contrast threshold is chosen to be 0.003, the sum of the attenuation and diffuse extinction coefficients as obtained from equations A.2, A.3, A.6 and A.8 is

$$k+\alpha = 1/D \ln [333 (\rho_D - u)/(u+w)] \qquad \text{A.9}$$

where

$$w = \rho_s \pi/(1-\rho_s)^2 \qquad \text{A.10}$$

When a glass bottomed viewer is used ($\rho_s = 0$), equation A.9 becomes

$$k+\alpha = 1/D \ln [333(\rho_D/u - 1)] \qquad \text{A.11}$$

For a constant value of u, Holmes[7] has determined that

$$D\ (k+\alpha) = \text{constant} = 9.4 \qquad \text{A.12}$$

In addition, the experimental data has been fitted to produce the equation

$$\alpha = \ln\ [100/(5.3D-3.4)] \qquad \text{A.13}$$

which is used to establish a relationship between k and α.

The α-meter provides accurate and repeatable measurements for a variety of operating conditions. A light source is focused to form a diffraction limited beam that is propagated through 1 meter of water. The light is detected by a small aperature photodetector. However, the finite spread of the beam in the conventional α-meter produces a value of α that is 25% lower than that obtained using an extremely narrow beam laser transmissometer. Another problem inherent with the conventional α-meter is the broad spectral filtering which is used on the detector. For the present measurement a narrow band (10 nm) interference filter was placed in front of the photodetector to enable measurements to be made of α as a function of wavelength.

The a-meter uses a ratio technique to measure the absorption by the water. A point source of light is placed between two detectors having wide fields of view. Each detector is a different distance from the point source so that the detecto

radiation of each detector is given by the equation

$$P_D(i) = P_s \frac{A_D}{4\pi D_i^2} e^{-aD_i} \qquad A.14$$

where

P_s = power of source

A_D = area of detector

D_i = distance between i^{th} detector and the point source

i = 1, 2 detector number

a = absorption coefficient

The absorption coefficient is then determined from equation A.15

$$(D_1 - D_2)\, a = [\ln \{P_D(1)/P_D(2)\} - 2 \ln (D_2/D_1)] \qquad A.15$$

This is accomplished electronically by a logarithmic amplifier. The values of D_1 and D_2 were chosen to be 1/3 and 2/3 meters respectively. Honey and Sorensen[8] have shown that accuracies better than 1% are achievable under moderate scattering conditions and accuracies of better than 7.5% are achievable for severe scattering conditions.

A set of measurements were made to compare the performance of the α-meter and the Secchi disk. This was accomplished by using the α-meter to measure the attenuation coefficient at 540 nm while observing a one foot diameter half-black half-white Secchi disk. The disk was moved away from the observer until it disappeared thereby defining the dis-

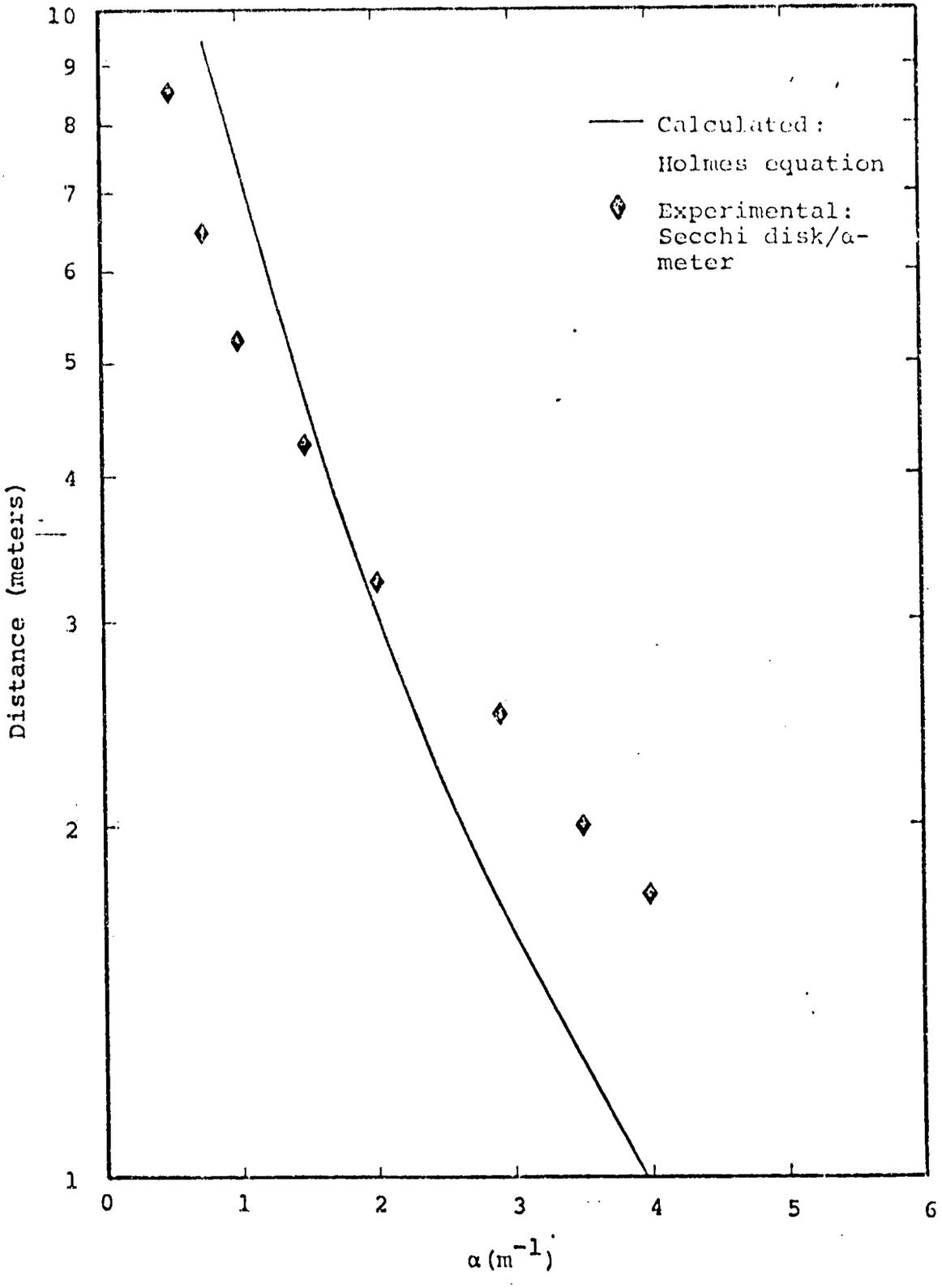

Figure A.1: Comparison of α-meter and Secchi disk visibility values.

tance D. For small and moderate α's this was done by moving the disk along the long dimension of the tank. For larger values of α the measurement was made by lowering the disk vertically into the water. In both cases a large fluorescent fixture was used to illuminate the disk. Shown in Figure A.1 is a plot of the experimental data along with Holmes' equation (A.13).

An inspection of this figure shows that for values of $\alpha \leq 2\ m^{-1}$, the difference between the measured and predicted values is $\Delta\alpha \simeq 0.5\ m^{-1}$. For larger values of α this difference becomes greater, i.e., $\Delta\alpha \simeq 1.0\ m^{-1}$. Possible sources of error are 1) the sun was the light source used in Holmes' experiments, whereas a standard fluorescent fixture was used in the present experiments, 2) differences in the intensity of the various sources and their spectral distributions.

Appendix B - Computer Program

The integrals expressed in equations (10) and (11) were integrated numerically using the Gauss-Simpson Rule. The integral

$$\int_a^b f(x)\ dx$$

can be represented by a summation

$$\int_a^b f(x)\ dx = h \sum_{m=0}^{n/2-1} \left\{ f(a+hk_1) + f(a+hk_2) \right\} \qquad (C.1)$$

for the values of n even and h=(b-a)/n where

$$k_1 = 1-1/\sqrt{3}+2m \qquad k_2 = 1+1/\sqrt{3}+2m \qquad (C.2)$$

The program used to evaluate equation C.1 is given below. The parameters used in the calculation are explained after the computer program.

Main Program

```
C=.2997
C2=C*C
D=1.650
A=.005
A2=A*A
ZIGMA=1.
P0=1.
EL=1.5
```

```
      GAMA=6.0
      ALPHA=1.
      N=10
      SN=N
      M=100
      HM=M
      CC=2.*3.1416*ZIGMA*P0/EL
      DO 1 J=1,6
      WRITE (6,41) ALPHA,GAMA
   41 FORMAT ('0','ALPHA=',F5.2,3X,'GAMA=',E13.3)
      T=D/C
      DO 2 I=1,N
      S=0.
      AL=(T-D/C)-GAMA
      IF (AL)  111,112,113
  111 TAMAX=0.5*(T-D/C)
      GO TO 114
  112 TAMAX=0.5*(T-D/C)
      GO TO 114
  113 TAMAX=GAMA
  114 HTA=TAMAX/HM
      A1=-1.577350
  100 TA=A1*HTA+2.*HTA
      LL=M/2
      DO 30 JL=1,LL
      F1=C2*((T-TA)**2)
      F1=A2+F1
      F1=SQRT(F1)
      F=C*(T-TA)
      F1=1.-F/F1
      F2=EXP(2.*ALPHA*C*TA)
      G1=4.*TA/GAMA-1.
      G1=-G1*G1
      G1=EXP(G1)
      Q=EXP(1.)
      QV=1./Q
      FM=Q/(Q-1.)
      G1=FM*(G1-QV)
      G1=G1*G1
      G2=CC*EXP(-2.*ALPHA*C*(T-D/C))
      ENT=C*F1*F2*G1*G2
      S=S+ENT
   30 TA=TA+2.*HTA
      IF (A1.NE.-1.577350) GO TO 44
      A1=A1+2./SQRT(3.)
      GO TO 100
   44 S=HTA*S
```

```
      WRITE (6,42) T,S
   42 FORMAT (' ','T=',E13.3,3X,'S=',E13.3)
    2 T=T+GAMA/SN
    1 ALPHA=ALPHA+1.
      CALL EXIT
      END
```

Program Parameters

C = velocity of light = 0.2997 m/nsec

D = distance between detector and water surface in meters

A = radius of the detector in meters

EL = pulse length in meters

P0 = total power in watts

ZIGMA = volume scattering function in the backwards direction

GAMA = pulse duration in nsec ——

ALPHA = attenuation coefficient of water in inverse meters

N = number of intervals that the pulse has been divided

M = number of terms in the summation

TA = integration variable

TAMAX = upper limit of integration

ENT = integrand

REFERENCES

1) Hickman, G. D., J. E. Hogg, E. J. Friedman and A. H. Ghovanlou, Oct. 1972, "Application of a Pulsed Laser for Measurements of Bathymetry and Algal Fluorescence," presented at the Eighth International Symposium on Remote Sensing of Environment at the University of Michigan.

2) Kim, H. H. and P. B. Mumola, April 1972, "Laser Induced Fluorescence for Rapid Mapping of Phytoplankton Distribution in the Sea," presented at the Annual Meeting of the Optical Society of America.

3) Jarrett, O., P. Mumola and C. Brown, June 1973, "Four Wavelength LIDAR Applied to Determination of Chlorophyll a Concentration and Algae Color Group," presented at the Remote Sensing of Water Resources International Symposium, Ontario, Canada.

4) Ghovanlou, A. H., G. D. Hickman and J. E. Hogg, March 1973, "Laser Transmission Studies of East Coast Waters," Sparcom Technical Report Number 2 on Contract N000-14-71C-0202.

5) Gilbert, G. D., Feb, 1970, "The Effect of Particle Size on Contrast Improvement and Polarization Discrimination for Underwater Targets," Applied Optics 9, No. 2.

6) Williams, J., 1970, "Optical Properties of the Sea," U.S. Naval Institute, Annapolis, Md.

7) Holmes, 1970, "Limnology and Oceanograph, 15, No. 5, p. 688.

8) Sorenson, G. and R. C. Honey, Feb 1968, "Underwater Visibility Meter Concept Study," SRI report. Contract N60530-67-C-0891.